Stem Cell Research 47 (2020) 101899

Contents lists available at ScienceDirect

Stem Cell Research

journal homepage: www.elsevier.com/locate/scr

# Extrinsic modulation of integrin α6 and progenitor cell behavior in mesenchymal stem cells

Nuria Nieto-Nicolau[a,b,d], Raquel M. de la Torre[b], Oscar Fariñas[a,d], Andrés Savio[a,d], Anna Vilarrodona[a,d], Ricardo P. Casaroli-Marano[a,b,c,d,*]

[a] Barcelona Tissue Bank (BTB) & Donor Center, Banc de Sang i Teixits (BST), Barcelona, Spain
[b] CellTec-UB, University of Barcelona, Barcelona, Spain
[c] Department of Surgery, School of Medicine & Hospital Clinic de Barcelona, University of Barcelona, Barcelona, Spain
[d] Institute of Biomedical Research Sant Pau (IIB-Sant Pau), Barcelona, Spain

ARTICLE INFO

*Keywords:*
Mesenchymal stem cells
Integrin alpha 6
Clonogenicity
Proliferation
Protein kinase B
Migration

ABSTRACT

Mesenchymal stem cells (MSC) are heterogeneous cells of complex nature that show different potentials while different culture conditions can modify their functionalities through interactions with the microenviroment. Here, we found that bone marrow (BM) MSC from different donor sources and passages that expressed higher levels of α6 integrin subunit (ITGA6), showed higher clonogenicity, migration and differentiation potential. ITGA6 showed important roles improving these potentials and regulating proliferation through protein kinase B (AKT) pathway and cell cycle inhibitor proteins p53 and p21. Moreover, ITGA6 downregulation impaired migration. Cell confluence regulated ITGA6, increasing its expression in low density cultures and decreasing in high density cultures. Besides, ITGA6- cells expressed ITGA6 when seeded at low densities. We found higher ITGA6 expression on fibronectin substrates at lower confluency. Fibronectin increased proliferation, clonogenicity, activation of AKT, decreased cell cycle inhibitor proteins and augmented growth factors expression. Spheres-derived MSC showed higher ITGA6 expression and enhanced potentials for migration, clonogenicity and proliferation. In conclusion, though there is an intrinsic regulation of ITGA6 expression, associated to the progenitor potential of BM-MSC, this expression is regulated by culture conditions and is translated in changes in cell behavior and proliferation. This knowledge could be used to enhance the potential of BM-MSC for clinical application.

## 1. Introduction

Mesenchymal stem cells (MSC) have emerged as a promising tool for tissue engineering because their capability to differentiate toward various lineages (Liu et al., 2009). These cells are also accessible somatic stem cells that can be easily isolated. Consequently, several clinical trials use MSC in disorders that need organ or tissue regeneration. This is the case of osteogenesis imperfecta, bone fractures, heart infarction, autoimmune disorders or graft-versus-host disease (Squillaro et al., 2016).

MSC are defined by plastic adherence, multilineage differentiation potential and a mesenchymal phenotype (Dominici et al., 2006). The phenotypic identification of MSC is based on the expression of CD73, CD90 and CD105 among other markers (Dominici et al., 2006) but none of these markers could identify progenitor phenotypes. However, MSC are a heterogeneous population of cells with different capabilities (Colter et al., 2001) and MSC from different donors or somatic sources can have different capacities (Alt et al., 2012; Zaim et al., 2012; Zhu et al., 2009). These issues can affect therapeutic results. So, it is necessary the search for markers that could distinguish the early progenitors of these cells and increase the knowledge of the intrinsic and extrinsic mechanisms modulating MSC progenitor behavior. Therefore, the characterization of optimal culture conditions to enhance the potential of MSC is of great significance.

*Abbreviations:* a-MSC, bone marrow mesenchymal stem cells from alive healthy donors; AT-MSC, adipose tissue mesenchymal stem cells; BM-MSC, bone marrow mesenchymal stem cells; CFE, colony forming efficiency; D+1, day one of culture; D+7, day seven of culture; ed-MSC, mesenchymal stem cells from cadaveric encephalic death donors; FN, fibronectin; ha-MSC, bone marrow mesenchymal stem cells from cadaveric heart arrest donors; ITGA6, integrin alpha 6; LN, laminin-111; P, passage number

* Corresponding author at: Department of Surgery, School of Medicine, University of Barcelona, Calle Sabino de Arana 1 (2nd floor – ophthalmology), E-08028 Barcelona, Spain.
*E-mail address:* rcasaroli@ub.edu (R.P. Casaroli-Marano).

https://doi.org/10.1016/j.scr.2020.101899
Received 11 March 2020; Received in revised form 11 June 2020; Accepted 24 June 2020
Available online 30 June 2020
1873-5061/ © 2020 The Author(s). Published by Elsevier B.V. This is an open access article under the CC BY-NC-ND license (http://creativecommons.org/licenses/BY-NC-ND/4.0/).

Stem cells are directed by the extracellular microenvironment, which modulates their self-renewal and differentiation. This requires a close interaction between stem cells and the signals arising from the niche (Bara et al., 2014). In this sense, integrins binding to extracellular matrix proteins can modulate stem cell behavior (Frith et al., 2012). Integrin alpha 6 (ITGA6) expression is conserved among different populations of stem cells, such as embryonic stem cells, epithelial intestine stem cells, neural stem cells and some MSC (Krebsbach and Villa-Diaz, 2017), and plays important functions regulating self-renewal (Villa-Diaz et al., 2016) and stemness (Lee et al., 2009; Yu et al., 2012). The interaction between microenvironmental signals and intrinsic cell cues are necessary for the preservation of progenitor potential and any shortcoming in this interaction is linked to a decrease in this potential. Increasing the knowledge between extrinsic and intrinsic cues would allow to improvements in the regenerative potential of MSC for cell therapy.

In this research, we aimed to determine whether the expression of ITGA6 could be modified extrinsically and whether this fact can influence the progenitor behavior of BM-MSC. To do so, we first considered the intrinsic expression of ITGA6 in MSC from different donor sources among passages and evaluated the implications of this integrin on proliferation, differentiation, migration and clonogenicity. Then, we studied the extrinsic modulation of ITGA6 expression through different substrates in low- and high-density cultures, exploring the impact in cell behavior. Finally, we explored a strategy to increase the expression of ITGA6 and the potentials of MSC for cell therapy using MSC spheroids. Our results suggest the existence of not only an intrinsic regulation of ITGA6 associated to the progenitor potential, but also a microenvironmental regulation of ITGA6 expression, that is translated in a modulation of cell cycle proteins, proliferation, differentiation, migration and clonogenicity.

## 2. Materials and methods

### 2.1. Ethical considerations

This study followed the ethical precepts of the Declaration of Helsinki (Fortaleza, Brazil, Oct 2013) and was approved by local ethics committee (CEIC, Hospital Clinic de Barcelona; Ref 7365-12). Human samples were processed according to guidance for clinical use (EEC regulations 2004/23/CE and 2006/17/CE) and to the legal requirements Spain (Law 14/2007, RD 1716/2011 and RD 9/2014). Samples were obtained under informed consent. The use of personal data complied with local regulations (Law/05/2018).

### 2.2. Isolation and culture of cells

BM-MSC were obtained by iliac crest bone marrow aspiration, and transmissible infections were excluded by serologic analyses. BM-MSC were isolated, as described elsewhere (Rider et al., 2008). BM-MSC were cultured in MSC medium comprising α minimum essential medium with GlutaMAX™ (αMEM-GT, Invitrogen, Carlsbad, CA) supplemented with non-inactivated 10% fetal calf serum (FCS, Invitrogen) and 1% antibiotics and maintained in 5% $CO_2$ at 37 °C. Same numbers of cells per donor were pooled at passage 1. Cells from 5 live healthy donors at passage 3 or 4 were used for experiments. When indicated, 3 different donor sources were used: alive healthy (a-MSC), cadaveric heart arrest (ha-MSC), and cadaveric encephalic death donors (ed-MSC). Isolation, culture, and characterization of adipose tissue MSC (AT-MSC) was showed previously (Martínez-Conesa et al., 2012). Doubling population time was calculated as described before (Piera-Velazquez et al., 2002). Induced pluripotent stem cells (IPSC) were kindly gifted by Angel Raya and used for qPCR experiments.

### 2.3. Spheroid and spheroid-derived MSC generation

For sphere formation, BM-MSC from healthy donors at passage 3–4 were plated at low density in ultralow-adherence 35 mm dishes (Invitrogen) in spheroid formation medium composed of DMEM/F12 (1:1)/ human endothelial serum-free medium (1:2) (Invitrogen), 15% chicken embryo extract (Seralab, Huissen, Netherland), 0.1 mM β-mercaptoethanol (Sigma), 1% nonessential amino acids (Sigma), 1% N2 and 2% B27 supplements (Invitrogen), 20 ng/ml recombinant human fibroblast growth factor (FGF)-basic, 20 ng/ml recombinant human epidermal growth factor (EGF), 20 ng/ml recombinant human platelet-derived growth factor (PDGF-AB), 20 ng/ml recombinant human oncostatin M (227 aa OSM, 20 ng/ml) and 40 ng/ml recombinant human IGF-1 (all supplements from Peprotech) and maintained as described (Isern et al., 2013). To generate spheroid-derived MSC, the MSC spheroids were seeded with MSC medium in adherent conditions, grown to the end of the passage, trypsinized, and used for experiments.

### 2.4. Multilineage differentiation experiments

Differentiation experiments were performed as described before (Mosna et al., 2010). Adipogenesis was performed with adipogenic induction medium containing Dulbecco's Modified Eagle's Medium 1 g/l (DMEM, Invitrogen) supplemented with 0.5 mM isobutyl methylxanthine (Sigma-Aldrich, Munich, Germany), 1 μM dexamethasone (Sigma-Aldrich), and 200 μM indomethacin (Sigma-Aldrich) and confirmed at 28 days by Oil-Red-O staining, eluted with 100% isopropanol. Osteogenic induction was performed in DMEM 1 g/l medium with 1 μM dexamethasone, 50 μg/mL ascorbic acid (Sigma-Aldrich), and 10 mM glycerol 2-phosphate (Sigma-Aldrich) and confirmed at 28 days by Alizarin Red staining, eluted with 10% cetylpyridinium chloride. Cells ($2 \times 10^5$ cells/$cm^2$) were pelleted and chondrogenic induction was performed adding DMEM 1 g/l supplemented with 0.4% insulin-transferrin-selenium (ITS, Sigma-Aldrich), 350 μM L-proline (Sigma-Aldrich), 170 nM ascorbic acid, 1 mM sodium pyruvate (Lonza, Verviers, Belgium) and 10 ng/ml transforming growth factor-beta 1 (TGF-β1, Sigma-Aldrich) for 28 days. After that, pellets were fixed with 4% paraformaldehyde for 1 h at room temperature, stained with Alcian Blue, embedded in paraffin, and sectioned at thicknesses of 5 μm.

### 2.5. Flow cytometry characterization and sorting

Cells were blocked with 10% FCS for 10 min and incubated for 30 min at room temperature with conjugated antibodies (Table S1). Samples were analyzed by FACS (Calibur Flow Cytometer, BD Biosciences, San José, CA, USA) and data were evaluated by Summit version 3.1 software (Cytomation, Fort Collins, CO, USA). ITGA6 analysis was performed at the end of the passages, unless indicated and size analysis was performed as described before (Romano et al., 2003). Sorting was performed in a FACS Aria Fusion cell sorting cytometer (BD Biosciences), and post-sorting vitality testing was done with trypan blue to ensure equal survival of the sorted populations. Mouse monoclonal IgG isotype antibody was used as a negative control (Table S1). To assay the influence of different substrates on ITGA6 expression, cells were seeded at a density of 1,000 cells/$cm^2$ on either fibronectin at 10 μg/mL (FN, Sigma-Aldrich), laminin-111 at 20 μg/mL (LN, Sigma-Aldrich, L2020, www.sigmaaldrich.com/catalog/product/sigma/l2020?lang=es&region=ES) or plastic. Cells were grown for 24 h (D + 1, low density) or 7 days (D + 7, high density). Cells were then trypsinized and subject to flow cytometry and clonogenic assay.

### 2.6. Colony forming efficiency assay

For clonogenic experiments, 10 cells/$cm^2$ were seeded in 35 mm diameter plates and cultured in MSC medium for 14 days. After that, cells were stained with 0.5% crystal violet. Colonies were scored

according to (Sotiropoulou et al., 2006). To test the influence of different substrates on the colony forming efficiency (CFE) potential, cells were seeded as described above.

### 2.7. Adhesion assay

For adhesion assays, 96 well plates were coated with specific extracellular adhesion proteins, FN at 10 μg/ml, LN at 20 μg/ml or bovine serum albumin (BSA, Sigma) at 10 μg/ml as a control. We seeded $10^4$ cells/cm$^2$ on coated plates in MSC medium. After the indicated time, wells were stained with 0.5% crystal violet, washed, air dried, and eluted with 33% acetic acid solution. Absorbance was measured with Tecan Infinite m200 pro (Tecan, Mannedorf). To test whether ITGA6 blocking could affect adhesion to the substrates, $5 \times 10^3$ cells were seeded with 10 μg/mL of an ITGA6 neutralizing antibody (Table S1) on the coated or uncoated 96-well plates, and adhesion assay was performed at 60 min. A mouse monoclonal IgG (Table S1) was used as a control.

### 2.8. Migration assay

Cell migration was analyzed using 24-well inserts with 8 μm pore size fluorescence blocking membranes (Corning, MA, USA) on 24-well plates. Cells were seeded in serum free medium (DMEM 1 g/l medium) in the insert. Culture medium with 10% FCS was added to the lower well and incubated for 20 h. The cells that migrated through the insert's membrane were stained using 5 μM Calcein (Molecular Probes™, Invitrogen) and their fluorescence was detected at an excitation of 480 nm and an emission of 530 nm (Tecan Infinite m200 pro). Cell migration was normalized to controls and expressed as a percentage of migration. The migrated cells were photographed in an epifluorescence microscope (BX61; Olympus R-FTL-T; Olympus America Inc., Center Valley, PA, USA), using the digital image acquisition program (Olympus DP Controller).

### 2.9. Proliferation assay

Proliferation was assayed by seeding $10^4$ cells/cm$^2$ on 96 wells in MSC medium, and a bromodeoxyuridine assay (BrdU) was added 24 h after cell seeding at a final concentration of 1 mM. After 2 h, DNA synthesis was assayed with the Cell Proliferation ELISA BrdU kit (Roche Molecular Biochemicals, Mannheim, Germany), according to manufacturer's instructions.

### 2.10. Small interfering mRNA transfection

To inhibit ITGA6 specifically, a small interfering mRNA (siRNA) knockdown assay was performed using a commercial ITGA6-targeting siRNA (sc-43129, Santa Cruz, CA, USA) with an unspecific siRNA (siCTL, sc-37007, Santa Cruz, CA, USA). The transfections were performed using Lipofectamine (Invitrogen) according to the manufacturer instructions. Briefly, cells were seeded at a density of 15,000 cells/cm$^2$, incubated with 2 μM siRNA, and lysed with a western blot loading buffer 72 h after transfection to evaluate protein expression.

### 2.11. Immunofluorescence and confocal microscopy

Cells grown on glass coverslips were fixed with 4% paraformaldehyde, permeabilized, and blocked. Coverslips were then incubated with primary antibodies for 16 h at 4 °C in a humidified chamber. After washes, proper secondary antibody was added for 60 min at 37 °C in a humidified chamber. The coverslips were mounted upside down with mounting medium (Vectashield, Vector Laboratories, CA, USA) and the nuclei were counterstained with DAPI (4′,6-diamidino-2-phenylindole). Cells were observed in an epifluorescence microscope. For confocal microscopy with MSC spheroids, spheres were treated as described above. Hoechst 33,342 (Sigma) was used for nucleus staining. Samples were mounted with Fluoromount (Sigma) and images were captured using a TCS SP2 Leica confocal laser scanning microscope (Leica Lasertechnick GmbH, Mannheim, Germany). Antibodies used are detailed in Table S1.

### 2.12. Western blot analysis

Western blot was performed as described before (Piera-Velazquez et al., 2002). Protein bands were revealed using an enhanced chemiluminescence substrate (Biological Industries, Reactiva, Barcelona, Spain) and recorded on autoradiography film (Kodak Rochester, NY, USA). Western blots were analyzed by digitally scanning the blots, and followed by densitometric analysis using ImageJ as indicated (Rasband, 2012). All analyses were normalized to a tubulin loading control, except for phosphorylated protein kinase B (p-AKT), which was normalized to the total AKT.

### 2.13. Extraction of mRNA and quantitative polymerase chain reaction

Total RNA was extracted from cells using a PureLink RNA Mini Kit (Ambion, Invitrogen), following manufacturer's instructions. The RNA concentration was measured using the Tecan Infinite m200 Pro, and 1 μg RNA was reverse-transcribed using Superscript III (Invitrogen), according to the manufacturer's instructions. Then, 0.5 μL of cDNA was used for quantitative polymerase chain reaction (qPCR) in a final volume of 18 μL with SYBR Green Reaction Mix (Invitrogen) and a 0.2 μM primer concentration. We performed qPCR using the Step One (Applied Biosystems, Life technologies, Glasgow, UK) hardware and software. The expression levels of target genes were normalized to internal 18 s (rrn18s, Tataa Biocenter, Sweden) and presented as relative expressions based on the $2^{-\Delta\Delta Ct}$ formula. Sequences and annealing temperatures of PCR primers are listed in Table S2.

### 2.14. Statistical analysis

Experiments were performed at least in triplicate. Two-tailed Student's *t*-tests were used for comparisons. Correlations were assessed using Kendall correlation coefficient (τ). Values of $p < 0.05$ were considered statistically significant. The R software, (R Development Core Team, 2012) was used. All results are presented as the mean ± standard error (MD ± SE).

## 3. Results

### 3.1. ITGA6 was related to higher clonogenicity and migration but was lost with culture passages

We first focused our attention on testing the intrinsic potentials of BM-MSC from distinct donor sources for clonogenicity, migration and ITGA6 expression at the end of different passages during amplification to determine whether ITGA6 could correlate with these potentials.

The highest ITGA6 expression was found in a-MSC and ha-MSC at passage number (P) 1, while ed-MSC showed the lowest expression. In all cases, ITGA6 levels decreased at P5 though a-MSC and ha-MSC shared similar expression levels and ed-MSC showed again the lowest expression (Fig. 1A). CFE assays at P1 revealed that a-MSC had the highest clonogenic capacity, followed by ha-MSC, whereas the ed-MSC showed the lowest capacity. CFE decreased with the passage number in all cases (Fig. 1B). However, a-MSC continued to exhibit higher CFE than ha-MSC while ed-MSC showed the lowest CFE at P5. To further study the correlation between ITGA6 expression and clonogenicity, we studied MSC from aged passages and other sources. So, we analyzed a-MSC at P9 and AT-MSC at P1 for CFE and ITGA6 expression (Fig. S1). Both presented insignificant CFE results that correlated with a very low expression of ITGA6. Kendall coefficient showed a strong correlation

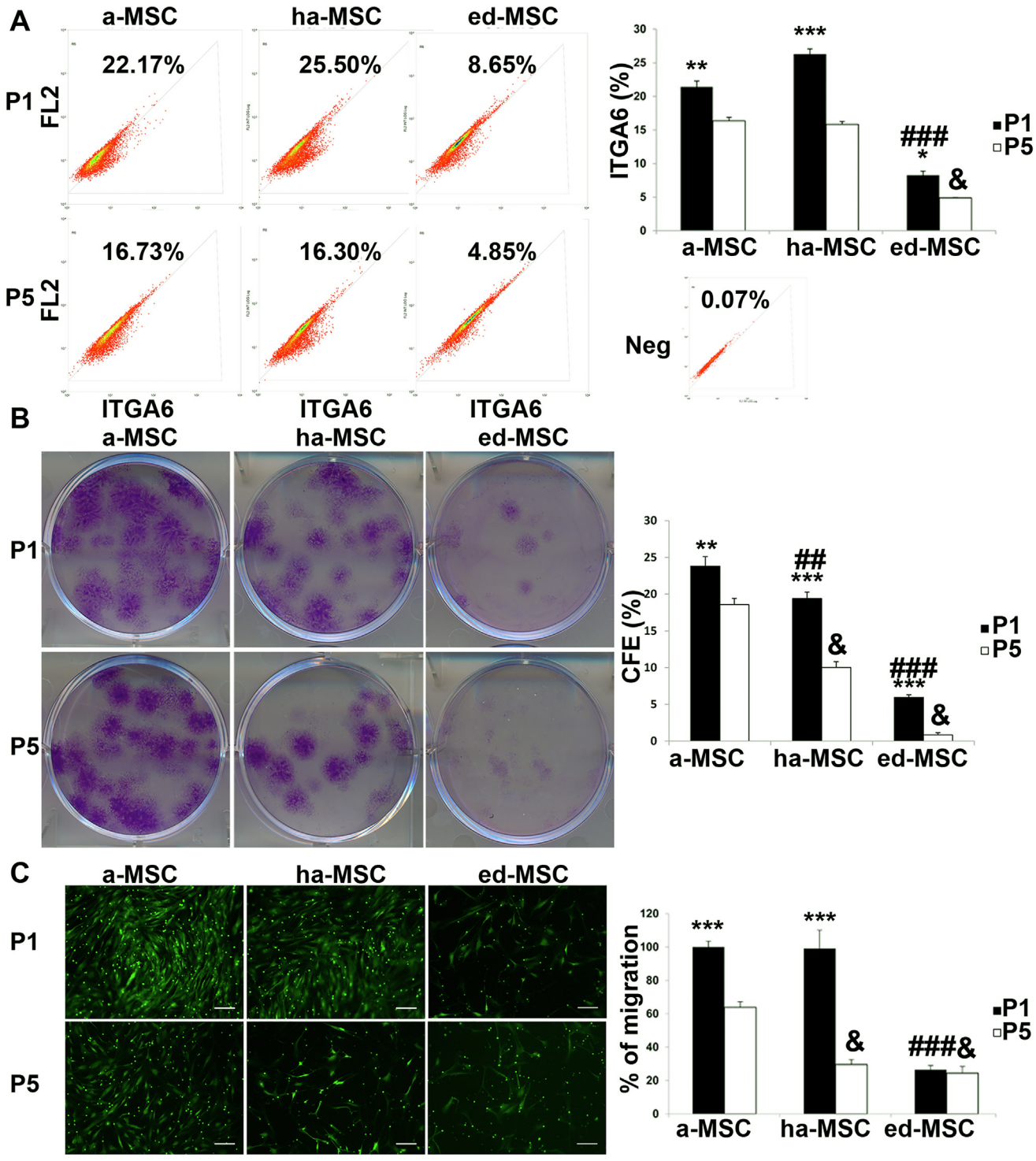


**Fig. 1.** ITGA6 expression, clonogenic and cell migration potential of BM-MSC from different sources. (A) Expression of ITGA6 + at passage 1 (P1) and 5 (P5) and isotype negative control (Neg). (B) Colony forming efficiency (CFE) assay at P1, P5. (C) transwell migration assays using calcein staining and the percent of migrated cells at P1 and P5 (Bar = 50 μm). BM-MSC from alive healthy (a-MSC), heart arrest (ha-MSC), and encephalic death (ed-MSC) donors. Results are presented as mean ± SE from 3 independent experiments. Statistical analysis was performed using two-tailed Student's *t*-tests (*, $p < 0.05$; **, $p < 0.01$; ***, $p < 0.001$ P1 compared to P5; ##, $p < 0.01$; ###, $p < 0.001$ compared to a-MSC P1; &, $p < 0.05$ compared to a-MSC).

between CFE and ITGA6 expression in all analyzed conditions ($\tau = 0.71$; $p = 0.003$) (Fig. S2).

Regarding migration, results showed similar patterns to those for CFE, decreasing with passage number. At P1, a-MSC and ha-MSC showed the highest percentages of migration, without significant differences, whereas ed-MSC group had the lowest percentage of migration. Thus, a-MSC and ha-MSC reduced its migration at P5, although ha-MSC highly reduced their potential. The percentage values of migration in ed-MSC were again the lowest (Fig. 1C).

### *3.2. MSC could retain mesenchymal phenotype although showed impaired clonogenicity or migration*

Next, to demonstrate the maintenance of mesenchymal phenotype,

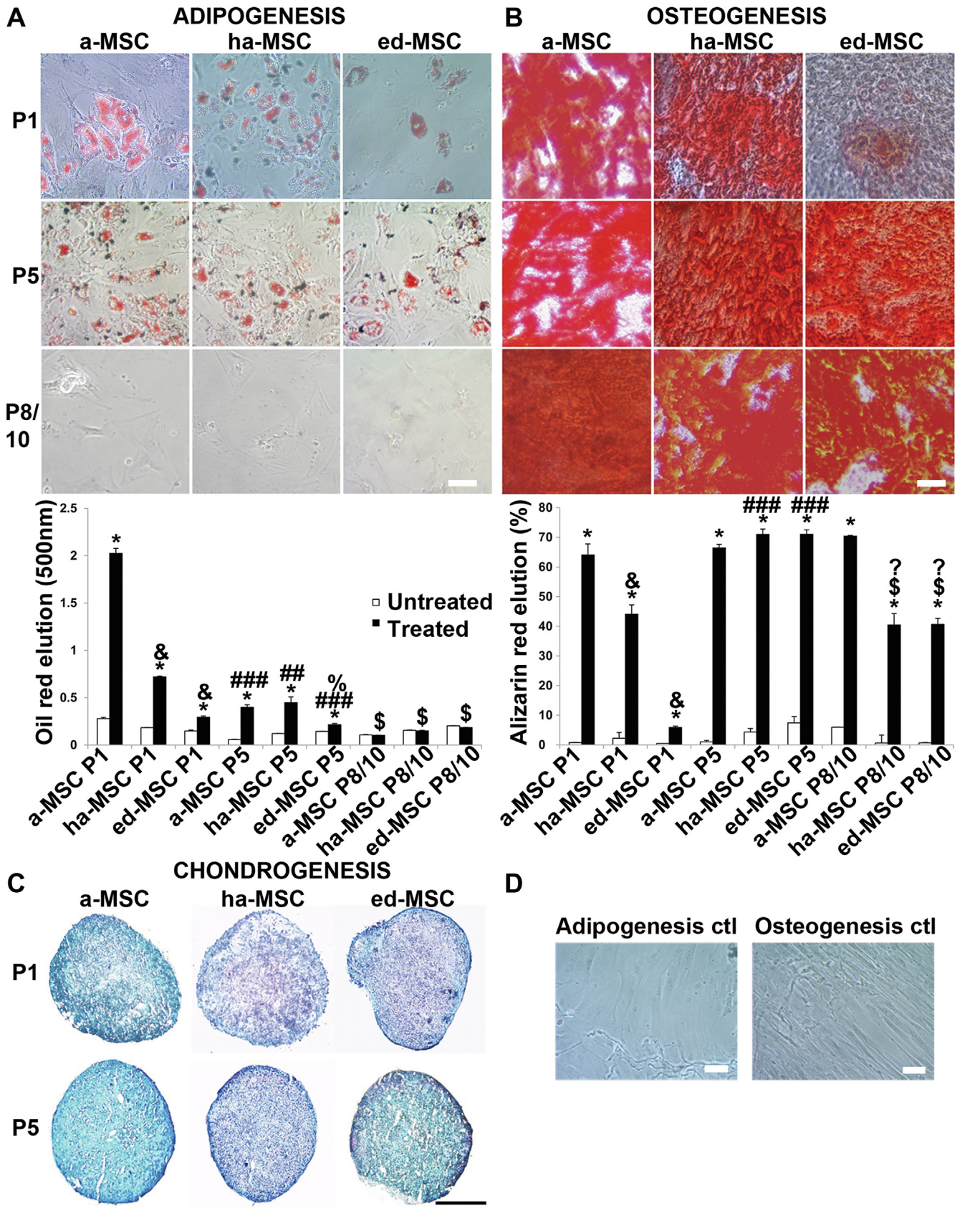


*(caption on next page)*

**Fig. 2.** Multi-lineage differentiation potential of BM-MSC from different sources. (A) *In vitro* adipogenesis differentiation at passage 1 (P1), 5 (P5) and 8–10 (P8/10) (Bar = 50 μm) and Oil Red staining elution quantification. (B) *In vitro* osteogenesis differentiation at P1, P5 and P8/10 (Bar = 50 μm) and Alizarin Red staining elution quantification. (C) *In vitro* chondrogenesis differentiation stained with Alcian Blue at P1, P5 and P8/10 (Bar = 200 μm). (D) Culture control conditions for adipogenesis and osteogenesis differentiation (Bar = 50 μm). BM-MSC from alive healthy (a-MSC), heart arrest (ha-MSC), and encephalic death (ed-MSC) donors. Results are presented as mean ± SE from 3 independent experiments. Statistical analysis was performed using two-tailed Student's *t*-tests (*, $p < 0.05$ treated compared to respective untreated controls in the same passage; &, $p < 0.05$ treated P1 compared to treated a-MSC at P1; ##, $p < 0.01$; ###, $p < 0.001$ treated P5 compared to respective treated P1; %, $p < 0.05$ ed-MSC P5 compared to a-MSC P5; $, $p < 0.05$ treated P8/10 compared to respective treated P5; ?, $p < 0.5$ treated P8/10 compared to treated a-MSC at P8/10).

we performed trilineage differentiation and phenotypic analysis for the MSC that were analyzed before for ITGA6 expression, CFE and migration at different passages.

All groups (a-, ed-, ha-MSC) successfully differentiated to osteogenic, adipogenic, or chondrogenic lineages during amplification up to P5, although there were differences in the differentiation potential (Fig. 2). Adipogenesis and osteogenesis were higher in a-MSC, followed by ha-MSC and ed-MSC had the lowest differentiation capacity at P1. Moreover, adipogenesis decreased through amplification while osteogenic differentiation was enhanced at P5. However, chondrogenesis and adipogenesis failed at P8/10. Further, the phenotypic characterization was maintained up to P5 in a-MSC. In the cadaveric donors, phenotypic characterization was lost at P5 (Table S3).

### 3.3. ITGA6 selected smaller BM-MSC with greater proliferation, clonogenicity and differentiation potentials

Then, we decided to check whether ITGA6 could be related to BM-MSC potentials. So, cell sorting assays or function-blocking antibodies were used to analyze proliferation, clonogenicity, differentiation and migration.

Sorted ITGA6 + cells showed increased proliferation compared with the ITGA6 − fraction (Fig. 3A). In addition, ITGA6 + cells showed augmented CFE and increased osteogenic and adipogenic differentiation potential (Fig. 3C–D). Moreover, ITGA6 function-blocked cells with specific antibodies presented reduced migration (Fig. 3F). Besides, we used flow cytometry to determine the differences in cell size of both fractions, showing that ITGA6 + cells were smaller than ITGA6 − cells (Fig. 3B).

### 3.4. Culture confluence regulated ITGA6 affecting proliferation

Next, we aimed to study the extrinsic modulation of ITGA6.To explore the effects of culture confluence on proliferation and ITGA6 expression, we purified ITGA6 + cells and ITGA6- cells by cell sorting, seeded them and compared them with unsorted cells. Then, we analyzed ITGA6 expression at 48 h and 168 h post-seeding. We also evaluated cell cycle proteins p53, p21 and the AKT pathway and calculated the doubling population time (DPT). To further explore the relationship between ITGA6 and cell cycle proteins, we performed mechanistic siRNA ITGA6 inhibition assays and analyzed the effects on cell cycle proteins.

At 48 h, almost all ITGA6 + fraction-derived cells expressed ITGA6 (Fig. 4A), while the unsorted cells expressed lessened ITGA6 expression. The ITGA6 + fraction-derived cells showed a very weak expression of p53 and p21 cell cycle inhibitor proteins and an increased proportion of the growth associated signal transduction pathway p-AKT (Fig. 4B). This correlated with decreased doubling population times (DPT), indicating higher proliferation (Fig. 4D). ITGA6- fraction-derived cells expressed ITGA6 although these levels were lower than in unsorted cells. ITGA6- fraction-derived cells showed the lowest AKT activation and the greatest increase of p53 and p21 (Fig. 4B), which correlated with higher DPT, indicating lower proliferation (Fig. 4D).

The expression of ITGA6 decreased with culture time in all the situations at 168 h, although ITGA6 + fraction-derived cells expressed higher levels of ITGA6, while ITGA6- fraction-derived cells expressed lower levels (Fig. 4A). At 168 h, the expression of p53, p21 and the AKT pathway were not different between all the situations (Fig. 4C). Although the DPT remained lower in the ITGA6 + fraction-derived cells, the DPT increased in all the situations in comparison with the DPT at 48 h (Fig. 4D). Collectively, these results showed a reduction in the proliferation until the end of the assay.

ITGA6 inhibited cells increased the expression cell cycle proteins p21, p27 and p53 (Fig. 4E). Accordingly, p-AKT was hindered, demonstrating the effect of ITGA6 on proliferation and supporting previous results (Fig. 3A).

### 3.5. Fibronectin enhanced more ITGA6 expression and CFE than laminin-111 at low densities

Then, to assay the possible influence of substrates on ITGA6, we assessed the changes in ITGA6 expression, CFE and migration induced by fibronectin or laminin-111 under different confluency conditions.

At day 1 (D + 1), cells seeded at low confluency on fibronectin expressed higher ITGA6 levels than either laminin-111 or controls as showed by flow cytometry (Fig. 5A and B) and immunofluorescence (Fig. 5C). There was an important reduction in ITGA6 expression 7 days after culture (D + 7) in all the situations. In fact, cells grown on fibronectin or laminin-111 showed more reduced ITGA6 expression than controls (Fig. 5A–C).

Cells seeded on fibronectin at low confluence demonstrated the highest CFE when reseeded on plastic (Fig. S3). BM-MSC grown on laminin-111 and fibronectin after 7 days led lesser CFE compared with controls. When examining the changes in cellular migration induced by confluence, cells had impaired migration at D + 7 compared with the cells seeded at D + 1 at lower confluence (Fig. S3).

### 3.6. Fibronectin improved more proliferation than laminin-111 activating AKT pathway

The influence of substrates was further studied testing cell proliferation on both laminin-111 and fibronectin at different times (24, 48 and 72 h) by BrdU incorporation assays and cell cycle proteins analysis.

Increased proliferation was seen at 24 h after the seeding, but the most enhanced proliferation was detected in cells grown on fibronectin, followed by those seeded on laminin-111 in comparison with controls (Fig. 6A). Surprisingly, the lowest p-AKT expression was detected on laminin-111 substrates (Fig. 6B). There was an increase in the proportion of p-AKT on fibronectin, indicating activation of the AKT pathway followed by controls. However, p21, p27, and p53 expressions were decreased on both laminin-111 and fibronectin compared with controls. Again, the lowest p21 and p27 expressions were found on fibronectin substrates, corroborating the BrdU incorporation results (Fig. 6B).

### 3.7. Laminin-111 was more specific for ITGA6 binding although fibronectin enhanced the expression of growth factors

To further understand the effects of substrates, we assayed the specificity of ITGA6 for binding laminin-111 or fibronectin and analyzed the migration of MSC towards these substrates. Moreover, we explored the mRNA expression of growth factors that could affect cell adhesion, proliferation, and migration.

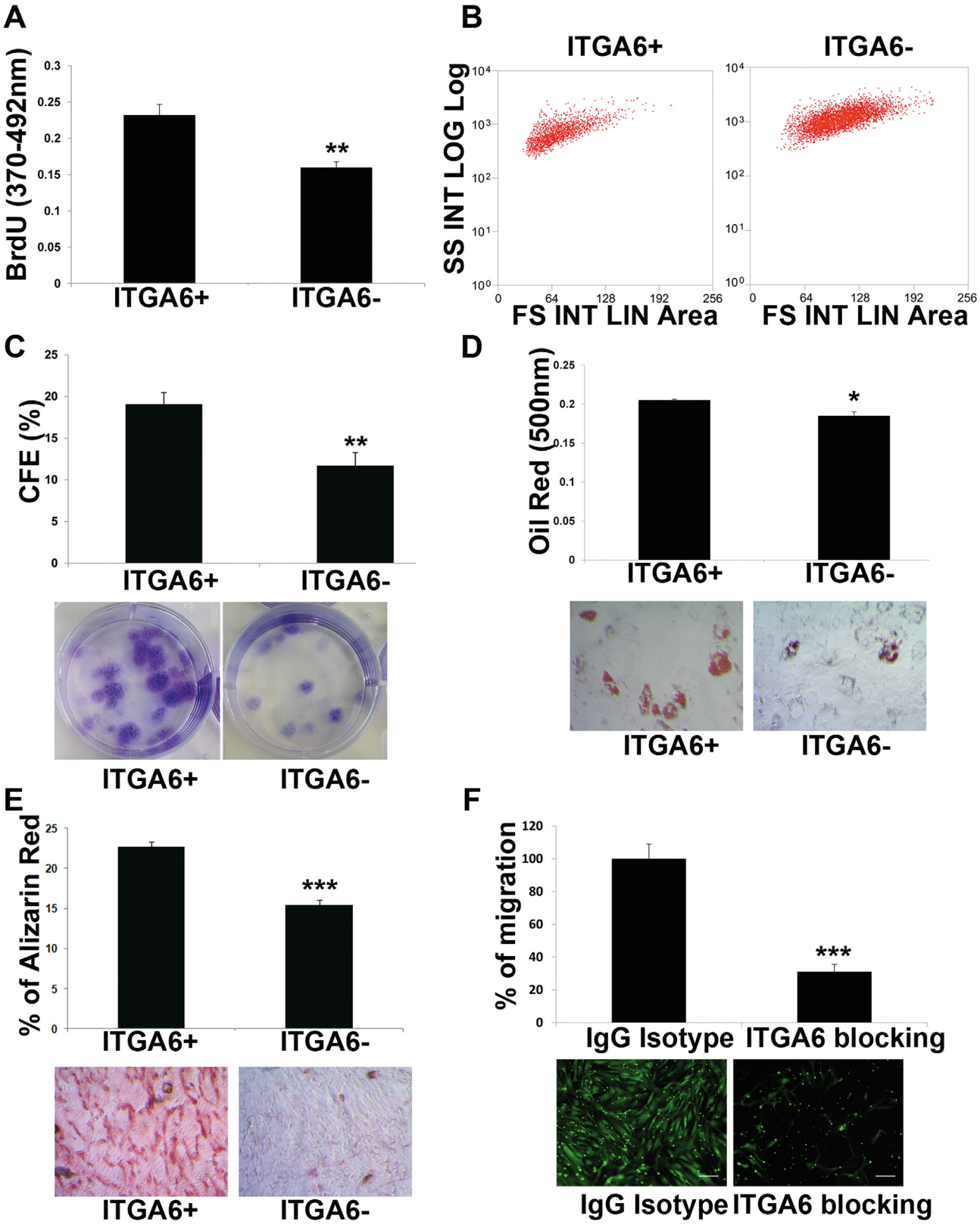


**Fig. 3.** ITGA6 expression and proliferative potential. (A) Analysis of proliferation between ITGA6 + and ITGA- sorted cells by bromodeoxyuridine (BrdU) incorporation assay. (B) Size analysis of ITGA6 + and ITGA6- sorted cell cultures by flow cytometry. (C) Colony forming efficiency (CFE) of ITGA6 + and ITGA6- sorted cell cultures. (D) *In vitro* adipogenesis differentiation and Oil Red staining elution quantification of ITGA6 + and ITGA6- sorted cell cultures. (E) *In vitro* osteogenesis differentiation and Alizarin Red staining elution quantification of ITGA6 + and ITGA6- sorted cell cultures. (F) Percent of migrated cells using ITGA6 blocking antibody compared to control cells (IgG isotype) using through transwell migration assays. Cells stained with (Bar = 50 μm). Results are presented as mean ± SE from 3 independent experiments. Statistical analysis was performed using two-tailed Student's *t*-tests (*, $p < 0.05$; **, $p < 0.01$; ***, $p < 0.001$).

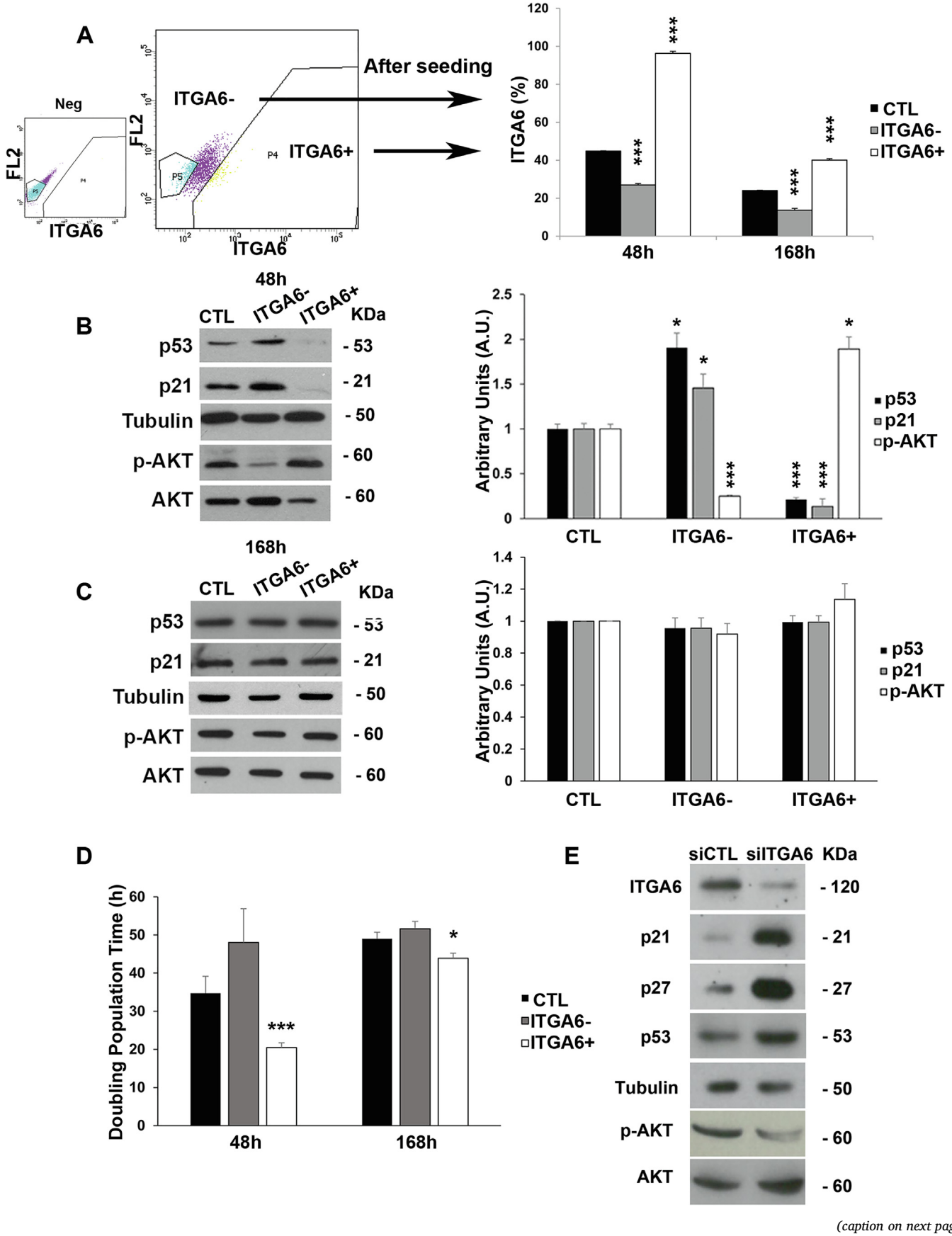


*(caption on next page)*

**Fig. 4.** ITGA6 regulation by culture confluence. (A) Sorting of both ITGA6 + and ITGA6- fractions by flow cytometry and the percent of ITGA6 of the both fractions and unsorted cells (CTL) after seeding them for 48 h and 168 h. (B) Western blot analysis and quantification for cell cycle proteins p53, p21 and AKT signaling pathway at 48 h after seeding. (C) Western blot analysis and quantification for cell cycle proteins p53, p21 and AKT signaling pathway at 168 h after seeding. (D) Doubling cell population times (DPT) of ITGA6 + , ITGA6- and CTL after being seeded for 48 h and 168 h. (E) Western blot analysis for cell cycle proteins and AKT in small interference mRNA transfected cells for ITGA6 inhibition (siITGA6), compared to control cells transfected with unspecific interference mRNA (siCTL). Results are presented as mean ± SE from 3 to 4 independent experiments. Statistical analysis was performed using two-tailed Student's *t*-tests (*, $p < 0.05$; **, $p < 0.01$; ***, $p < 0.001$).

Cell adhesion on laminin-111 decreased at every time point (10, 20, 30, and 60 min) (Fig. 6C), while adhesion on fibronectin increased at 10 min and 30 min. Using an ITGA6 function-blocking antibody, cell adhesion was lowered on the laminin-111 substrate, indicating a specific participation of laminin-111 binding in MSC (Fig. 6E). Improved migration from the apical to the basal side was observed on both the laminin-111 -and fibronectin-coated inserts (Fig. 6F).

The mRNA expressions of epidermal growth factor receptor (*EGFR*), transforming growth factor β (*TGF-β*), matrix metalloproteinase 2 (*MMP2*), and interleukin 6 (*IL-6*) increased in cells seeded on fibronectin for 24 h (Fig. 6D). Only *MMP2* and *IL-6* expressions were increased in cultures grown on laminin-111 for 24 h.

### 3.8. Spheroid-derived MSC presented higher ITGA6 expression, proliferation, greater p-AKT activation and improved progenitor markers expression

Finally, we explored a strategy to increase MSC potentials. To do so,

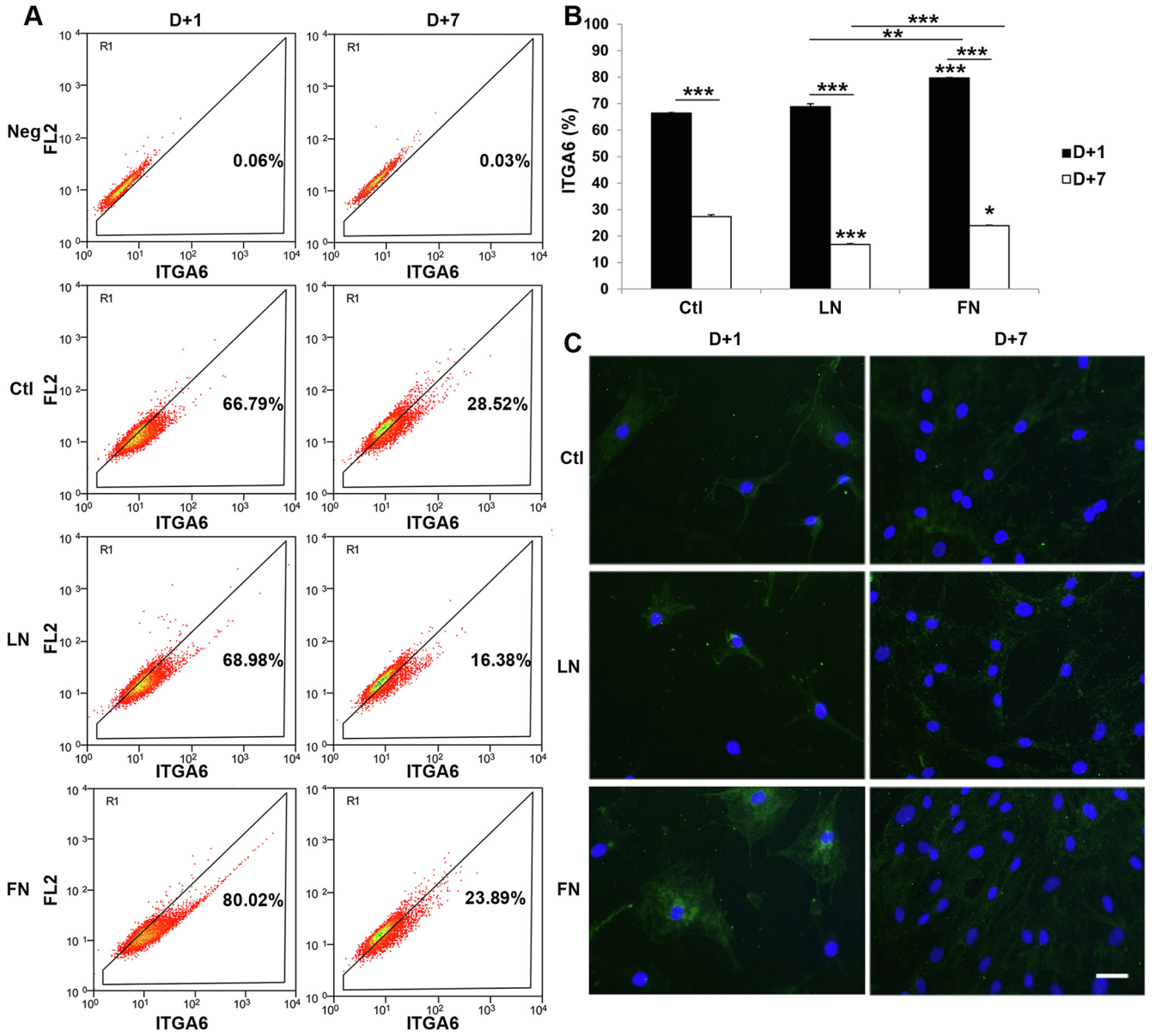


**Fig. 5.** ITGA6 expression on different substrates and the effects of culture confluence. (A–B) ITGA6 expression in BM-MSC by FACS on the different substrates at low (D + 1) and high (D + 7) confluence cell culture conditions. Isotype negative controls (Neg). (C) Immunofluorescence for ITGA6 staining in BM-MSC on Ctl, LN and FN at low (D + 1) and high (D + 7) confluence (Bar = 20 μm). Results are presented as mean ± SE from 3 independent experiments. Statistical analysis was performed using two-tailed Student's *t*-tests (*, $p < 0.05$; **, $p < 0.01$; ***, $p < 0.001$).

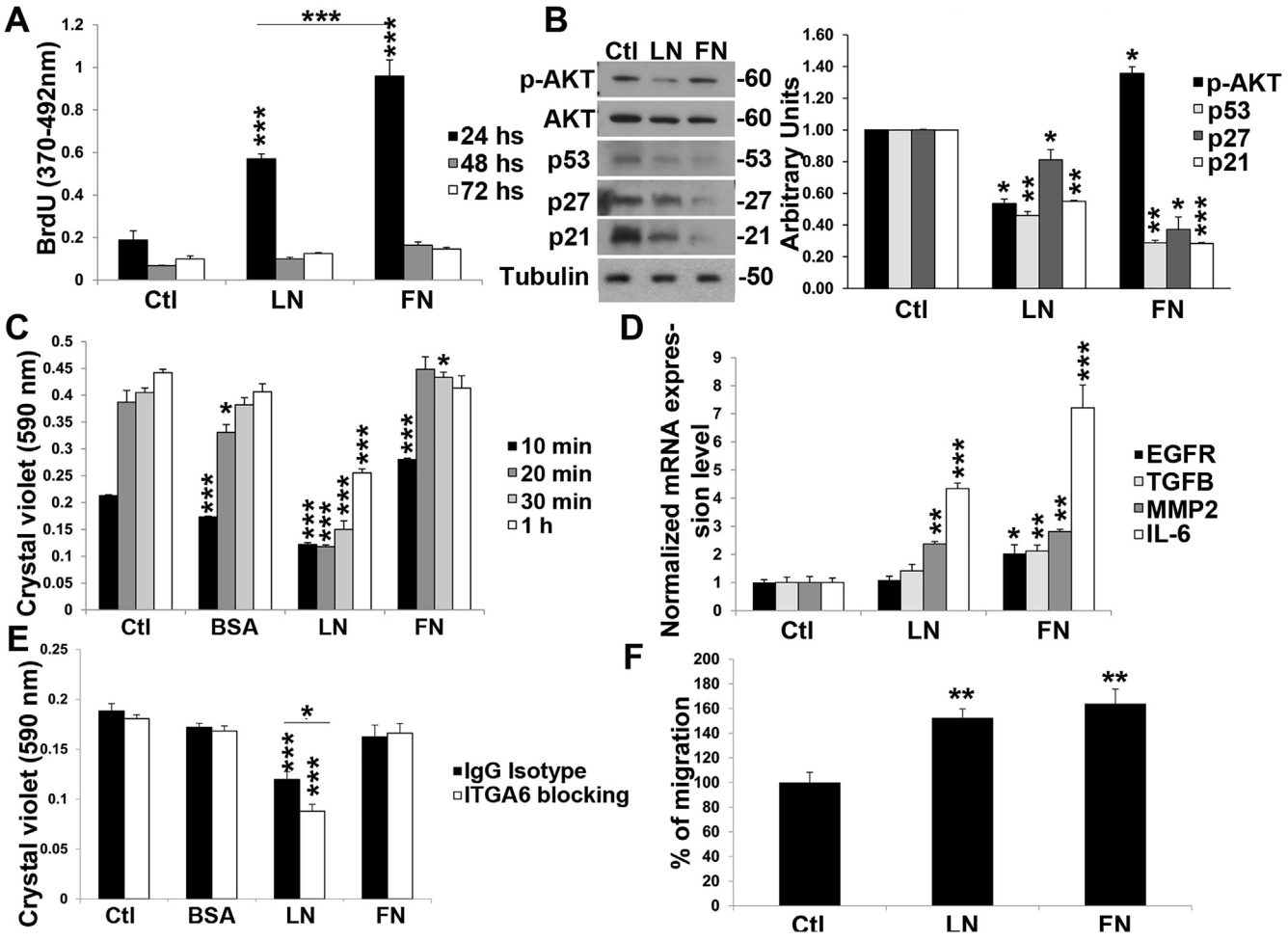


**Fig. 6.** Implications of different substrates in BM-MSC behavior. (A) Cell proliferation assay by bromodeoxyuridine (BrdU) on laminin-111 (LN) and fibronectin (FN), and plastic (Ctl). (B) Western blot analysis for p21, p27 and p53 and AKT on LN and FN. (C) Cell adhesion assay on extracellular matrix proteins LN, FN, bovine serum albumin (BSA) and Ctl. (D) Expression of *EGFR*, *TGF-β*, *MMP2* and *IL-6* mRNA in BM-MSC by qPCR on LN, FN and Ctl. (E) Cell adhesion assay on LN, FN and BSA with (ITGA6 blocking) and without (IgG isotype) blockage on different substrates. (F) Percent of migrated cells trough transwells coated with LN and FN. Results are presented as mean ± SE from 3 independent experiments. Statistical analysis was performed using two-tailed Student's *t*-tests (*, $p < 0.05$; **, $p < 0.01$; ***, $p < 0.001$).

we generated spheroids under non-adherent conditions, seeded them (spheroid-derived MSC), analyzed the expression of ITGA6 and their capacities using as controls monolayer cultured MSC at the same passage (Ctl). In these experiments we evaluated the migration potential, the proliferation, the clonogenicity and the mRNA expression levels of *SOX2*, *OCT4* and *NANOG*. Since MSC express low or negligible levels of Sox2 and Oct4 (Han et al., 2014; Matic et al., 2016; Pierantozzi et al., 2011), we hypothesized that any increase in these pluripotency factors could be linked to a higher progenitor state (Boiani and Schöler, 2005; Orkin et al., 2008). IPSC were used for comparison.

Spheroid-derived MSC expressed more ITGA6 than monolayer-derived MSC at the same passage (Fig. 7A). Moreover, the spheroid-derived MSC showed increased CFE, migration potential, and improved proliferation (Fig. 7B–D). Thus, the highest levels of p-AKT were present in MSC spheroids followed by spheroid-derived MSC (Fig. 7E). Proliferating cell nuclear antigen (PCNA) was higher in spheroid-derived MSC and MSC spheroids and cell cycle inhibitor protein p27 was downregulated in both conditions. Moreover, a marked upregulation in the mRNA expression levels of the *SOX2*, *OCT4* and *NANOG* were noted in MSC spheroids (Fig. 7F). MSC spheroids expressed similar levels of *SOX2* and *NANOG* than those expressed by IPSC, although IPSC showed higher expression of *OCT4*. Spheroid-derived MSC downregulated the expression levels of the pluripotency factors, though retained higher expression of *OCT4* and *SOX2* than the controls, monolayer cultured MSC. However, spheroid-derived MSC showed lower levels of *NANOG*. Increases in Sox2 and Oct4 could be also noticed in spheroid-derived MSC compared with controls in representative micrographs by immunofluorescence (Fig. 7G).

## 4. Discussion

In this study, we showed that ITGA6 expression is associated to intrinsic progenitor potentials and that could be upregulated extrinsically by cell culture microenvironment, improving the proliferation, migration and clonogenicity while activated AKT pathway and decreased cell cycle inhibitor proteins.

CFE is a widely accepted assay for quantifying the number of progenitor cells in MSC cultures (Cordeiro-Spinetti et al., 2014) and for predicting the replicative potential (Digirolamo et al., 1999). BM-MSC with higher CFE, migration and differentiation potentials were those expressing more ITGA6, and those potentials as well as ITGA6 were lost during passage amplification, even if MSC retained mesenchymal phenotype. In agreement, we demonstrated that ITGA6 + cells had increased CFE, supporting previous research (Lee et al., 2009; Yu et al., 2012) and that a discrete reduction in ITGA6 expression can hinder CFE. Cell size and progenitor potential are related in MSC, with smaller cells showing enhanced potential for differentiation and rapid self-renewal (Colter et al., 2001). Our findings pointed out that ITGA6 + cells

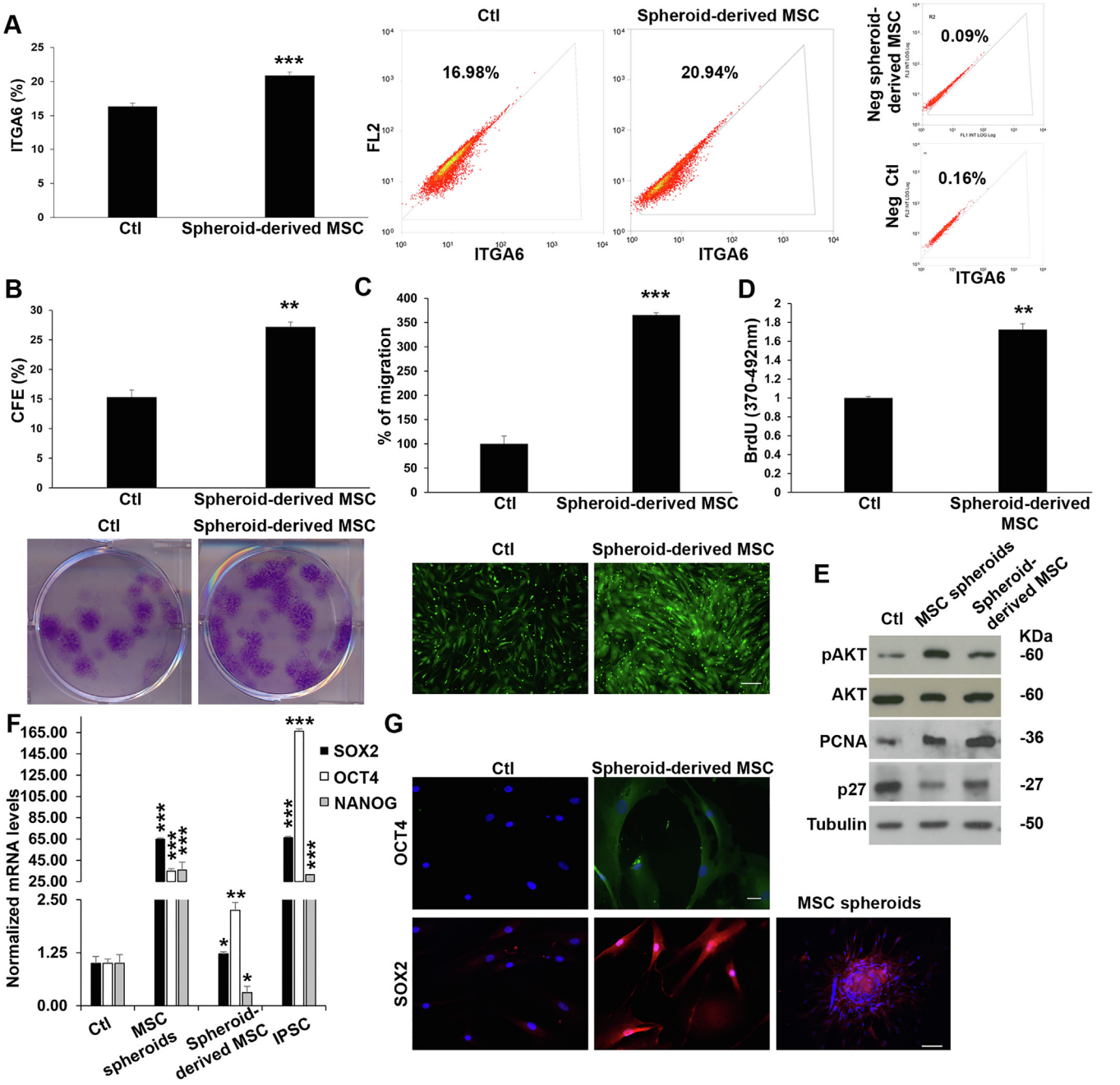


**Fig. 7.** Stemness potential, proliferation and migration of ITGA6 + spheroid-derived MSC. (A) Expression of ITGA6 in spheroid-derived MSC by FACS analysis compared to monolayer control cells (Ctl) and isotype negative controls (Neg). (B) Colony forming efficiency (CFE). (C) Transwell migration assay using calcein staining and the percent of migrated spheroid-derived MSC (Bar = 50 μm). (D) Spheroid-derived MSC proliferation capability by bromodeoxyuridine (BrdU) incorporation assay. (E) Western blot analysis p27, PCNA and AKT cell signaling pathway in MSCm/p, MSCm and (Ctl). (F) Expression of *SOX2* and *OCT4* mRNA in spheroid-derived MSC, spheroid and Ctl by qPCR. (G) Representative immunofluorescence micrographs for SOX2 and OCT4 in spheroid-derived MSC and Ctl (Bar = 20 μm). Results are presented as mean ± SE from 3 independent experiments. Statistical analysis was performed using two-tailed Student's *t*-tests (*, $p < 0.05$; **, $p < 0.01$; ***, $p < 0.001$).

were smaller and had an increased differentiation capacity, supporting the greater progenitor potential of this fraction. Our data suggests that ITGA6 is regulated by an intrinsic program that indicates the progenitor potential of each BM-MSC. So, ITGA6 could be a candidate for predicting MSC progenitor potential. Further, we confirmed that ITGA6 increased proliferation through AKT and cell cycle inhibitor proteins p53, p27, and p21 agreeing with previous reports in umbilical cord blood MSC (Yu et al., 2012).

MSC seeded at low density can increase progenitor gene expression such as *OCT4* and *NANOG* (Lee et al., 2013, 2009). In agreement, we showed that ITGA6 expression decreased as confluency increased, confirming the microenvironmental regulation of this integrin. So, the decrease in proliferation in high confluent cultures was related to the change in the expression of ITGA6 and the regulation of AKT pathway and cell cycle inhibitor proteins, pointing out that the ITGA6 can act as a proliferation regulator in response to culture confluence. ITGA6 was expressed in cultures from ITGA6-cells, showing that lower confluences can induce ITGA6 expression, further indicating the extrinsic modulation of ITGA6 expression by culture confluence.

Levels of ITGA6 and CFE increased on cells grown for 1 day at low

confluence on fibronectin, though ITGA6 was more specific for laminin-111 binding than fibronectin, which suggests that fibronectin could favor progenitor potential in MSC at low densities in comparison with laminin-111. Although, further research is needed to clarify the exact mechanism through fibronectin could increase ITGA6 expression, there was an improved BM-MSC proliferation on fibronectin by AKT activation and a decrease of cell cycle inhibitor proteins. More studies are needed also to study the effects of other laminin isoforms, though laminin-111 increased proliferation through impaired expressions of cell cycle inhibitor proteins, but not by AKT activation, which was inhibited. Overall, our data suggest a bilateral interplay between AKT pathway and ITGA6 expression. So, our results from ITGA6 mechanistic assays and substrate-seeding analyses indicate that AKT pathway activation can play a central role in ITGA6 expression, supporting previous data (Yu et al., 2012). To note, MSC treatment with TGF-β increases ITGA6 expression (Shangguan et al., 2012), which is consistent with our results showing that *TGF*-β was only increased on fibronectin substrates where ITGA6 was augmented. Moreover, EGFR is known to activate the AKT signaling pathway (Garay et al., 2015; Huang et al., 2013; Krampera et al., 2005; Tamama et al., 2006), expression that was increased on fibronectin, where AKT signaling pathway was activated. Moreover, the highest *IL*-6 expression was found also in fibronectin substrates, and IL-6 acts as a growth factor for MSC which deficiency decreases the MSC progenitors *in vivo* (Rodríguez et al., 2004). Therefore, these results could provide new insights about ITGA6 regulation.

More studies are needed regarding MSC migration and homing (Ullah et al., 2019). Here, we showed that when ITGA6 decreased or was functionally inhibited, migration of BM-MSC was impaired. This is consistent with previous *in vivo* reports showing that ITGA6 blockade reduces the homing of hematopoietic progenitors to the bone marrow (Qian et al., 2006). Also, PODXL$^{hi}$/ITGA6$^{hi}$ MSC population increased cell migration toward an infarcted heart in mice (Lee et al., 2009). So, we can posit that changes in the migration results induced by low confluence and high confluence cultures are mediated, at least in part, by ITGA6.

The spheroid microenvironment can enrich a culture in progenitor stem cells (Zhang et al., 2015). The generation of spheroids is mediated by ITGA6 through increases in *OCT4* and *SOX2*, which control its transcriptional regulation (Yu et al., 2012). Here, we showed that these increases can be comparable to the expression levels of these factors in IPSC, suggesting a high increase of the progenitor potential, since these factors are central core players in maintaining self-renewal and pluripotency (Rizzino, 2013). We also showed that spheroid-derived MSC retained, to some extent, augmentation of these pluripotency markers compared with controls, although *NANOG* was downregulated. However, *NANOG* is not essential to maintain multipotency (Marthaler et al., 2016). So, the increase of *SOX2* and *OCT4* in spheroid-derived MSC was translated into increased ITGA6 expression, higher CFE, a greater proliferation and improved migration results. Such an approach could enhance the potential of BM-MSC and could be used *in vitro* to increase their therapeutic efficacy for clinical application.

## 5. Conclusions

Our results point out that although there is an intrinsic program regulating the expression of ITGA6, which can indicate the progenitor potential of BM-MSC, specific culture conditions and extracellular matrix proteins modulate ITGA6 expression. This affects the proliferation, through AKT signaling pathway and cell cycle inhibitor proteins, as well as CFE and migration. These conditions could be used to enhance the progenitor potential of MSC in cell therapy approaches.

## CRediT authorship contribution statement

**Nuria Nieto-Nicolau:** Conceptualization, Data curation, Investigation, Methodology, Formal analysis, Validation, Writing - original draft, Writing - review & editing. **Raquel M. Torre:** Data curation, Investigation. **Oscar Fariñas:** Resources. **Andrés Savio:** Resources. **Anna Vilarrodona:** Resources. **Ricardo P. Casaroli-Marano:** Conceptualization, Methodology, Supervision, Visualization, Project administration, Funding acquisition, Writing - review & editing.

## Declaration of Competing Interest

The authors declare that they have no known competing financial interests or personal relationships that could have appeared to influence the work reported in this paper.

## Acknowledgments

This work was funded in part by a grant from Fondos de Investigaciones Sanitarias del Instituto Carlos III (FIS14-PI00196 and FIS18-PI00355) and Fundació Marató TV3 (20120630-30-31), and co-financed by the European Regional Development Fund (FEDER) of the European Union (EC).

## Appendix A. Supplementary data

Supplementary data to this article can be found online at https://doi.org/10.1016/j.scr.2020.101899.

## References

Alt, E.U., Senst, C., Murthy, S.N., Slakey, D.P., Dupin, C.L., Chaffin, A.E., Kadowitz, P.J., Izadpanah, R., 2012. Aging alters tissue resident mesenchymal stem cell properties. Stem Cell Res. 8, 215–225. https://doi.org/10.1016/j.scr.2011.11.002.

Bara, J.J., Richards, R.G., Alini, M., Stoddart, M.J., 2014. Concise review: bone marrow-derived mesenchymal stem cells change phenotype following in vitro culture: implications for basic research and the clinic. Stem Cells 32, 1713–1723. https://doi.org/10.1002/stem.1649.

Boiani, M., Schöler, H.R., 2005. Regulatory networks in embryo-derived pluripotent stem cells. Nat. Rev. Mol. Cell Biol. doi:10.1038/nrm1744.

Colter, D.C., Sekiya, I., Prockop, D.J., 2001. Identification of a subpopulation of rapidly self-renewing and multipotential adult stem cells in colonies of human marrow stromal cells. Proc. Natl. Acad. Sci. USA 98, 7841–7845. https://doi.org/10.1073/pnas.141221698.

Cordeiro-Spinetti, E., de Mello, W., Trindade, L.S., Taub, D.D., Taichman, R.S., Balduino, A., 2014. Human bone marrow mesenchymal progenitors: perspectives on an optimized in vitro manipulation. Front. Cell Dev. Biol. 2, 1–8. https://doi.org/10.3389/fcell.2014.00007.

Digirolamo, C.M., Stokes, D., Colter, D., Phinney, D.G., Class, R., Prockop, D.J., 1999. Propagation and senescence of human marrow stromal cells in culture: a simple colony-forming assay identifies samples with the greatest potential to propagate and differentiate. Br. J. Haematol. 107, 275–281. https://doi.org/10.1046/j.1365-2141.1999.01715.x.

Dominici, M., Le Blanc, K., Mueller, I., Slaper-Cortenbach, I., Marini, F., Krause, D., DeansKeating, R., Prockop, D., Horwitz, E., 2006. Minimal criteria for defining multipotent mesenchymal stromal cells. The International Society for Cellular Therapy position statement. Cytotherapy 8, 315–317. https://doi.org/10.1080/14653240600855905.

Frith, J.E., Mills, R.J., Hudson, J.E., Cooper-White, J.J., 2012. Tailored integrin-extracellular matrix interactions to direct human mesenchymal stem cell differentiation. Stem Cells Dev. 21, 2442–2456. https://doi.org/10.1089/scd.2011.0615.

Garay, C., Judge, G., Lucarelli, S., Bautista, S., Pandey, R., Singh, T., Antonescu, C.N., 2015. Epidermal growth factor-stimulated Akt phosphorylation requires clathrin or ErbB2 but not receptor endocytosis. Mol. Biol. Cell 26, 3504–3519. https://doi.org/10.1091/mbc.E14-09-1412.

Han, S.M., Han, S.H., Coh, Y.R., Jang, G., Ra, J.C., Kang, S.K., Lee, H.W., Youn, H.Y., 2014. Enhanced proliferation and differentiation of Oct4- And Sox2-overexpressing human adipose tissue mesenchymal stem cells. Exp. Mol. Med. 46, e101–e109. https://doi.org/10.1038/emm.2014.28.

Huang, C.K., Tsai, M.Y., Luo, J., Kang, H.Y., Lee, S.O., Chang, C., 2013. Suppression of androgen receptor enhances the self-renewal of mesenchymal stem cells through elevated expression of EGFR. Biochim. Biophys. Acta - Mol. Cell Res. 1833, 1222–1234. https://doi.org/10.1016/j.bbamcr.2013.01.007.

Isern, J., Martín-Antonio, B., Ghazanfari, R., Martín, A.M., López, J.A., del Toro, R., Sánchez-Aguilera, A., Arranz, L., Martín-Pérez, D., Suárez-Lledó, M., Marín, P., Van Pel, M., Fibbe, W.E., Vázquez, J., Scheding, S., Urbano-Ispizúa, Á., Méndez-Ferrer, S., Aslan, H., Zilberman, Y., Kandel, L., Liebergall, M., Oskouian, R.J., Gazit, D., Gazit, Z., Baksh, D., Davies, J.E., Zandstra, P.W., Boitano, A.E., Wang, J., Romeo, R., Bouchez, L.C., Parker, A.E., Sutton, S.E., Walker, J.R., Flaveny, C.A., Perdew, G.H., Denisonal, M.S., Bonzon-Kulichenko, E., Martínez-Martínez, S., Trevisan-Herraz, M., Navarro, P., Redondo, J.M., Vázquez, J., Breems, D.A., Blokland, E.A., Ploemacher,

R.E., Broxmeyer, H.E., Campbell, T.B., Hangoc, G., Liu, Y., Pollok, K., Broxmeyer, H.E., Christopherson, K.W., Paganessi, L.A., Napier, S., Porecha, N.K., de Lima, M., McNiece, I., Robinson, S.N., Munsell, M., Eapen, M., Horowitz, M., Alousi, A., Saliba, R., McMannis, J.D., Kaur, I., Delaney, C., Heimfeld, S., Brashem-Stein, C., Voorhies, H., Manger, R.L., Bernstein, I.D., Maggio, N Di, Mehrkens, A., Papadimitropoulos, A., Schaeren, S., Heberer, M., Banfi, A., Martin, I., Ding, L., Saunders, T.L., Enikolopov, G., Morrison, S.J., Ferraro, F., Lymperi, S., Méndez-Ferrer, S., Saez, B., Spencer, J.A., Yeap, B.Y., Masselli, E., Graiani, G., Prezioso, L., Rizzini, E.L., Friedenstein, A.J., Chailakhjan, R.K., Lalykina, K.S., Goessling, W., Allen, R.S., Guan, X., Jin, P., Uchida, N., Dovey, M., Harris, J.M., Metzger, M.E., Bonifacino, A.C., Stroncek, D., Harvey, K., Dzierzak, E., Hoggatt, J., Singh, P., Sampath, J., Pelus, L.M., Kawada, H., Ando, K., Tsuji, T., Shimakura, Y., Nakamura, Y., Chargui, J., Hagihara, M., Itagaki, H., Shimizu, T., Inokuchi, S., Larsson, J., Karlsson, S., Méndez-Ferrer, S., Lucas, D., Battista, M., Frenette, P.S., Méndez-Ferrer, S., Michurina, T.V., Ferraro, F., Mazloom, A.R., Macarthur, B.D., Lira, S.A., Scadden, D.T., Ma'ayan, A., Enikolopov, G.N., Frenette, P.S., Mercier, F.E., Ragu, C., Scadden, D.T., Mignone, J.L., Kukekov, V., Chiang, A.S., Steindler, D., Enikolopov, G., Nilsson, S.K., Johnston, H.M., Whitty, G.A., Williams, B., Webb, R.J., Denhardt, D.T., Bertoncello, I., Bendall, L.J., Simmons, P.J., Haylock, D.N., North, T.E., Goessling, W., Walkley, C.R., Lengerke, C., Kopani, K.R., Lord, A.M., Weber, G.J., Bowman, T.V., Jang, I.H., Grosser, T., Notta, F., Doulatov, S., Laurenti, E., Poeppl, A., Jurisica, I., Dick, J.E., Omatsu, Y., Sugiyama, T., Kohara, H., Kondoh, G., Fujii, N., Kohno, K., Nagasawa, T., Pajtler, K., Bohrer, A., Maurer, J., Schorle, H., Schramm, A., Eggert, A., Schulte, J.H., Robinson, S.N., Simmons, P.J., Thomas, M.W., Brouard, N., Javni, J.A., Trilok, S., Shim, J.S., Yang, H., Steiner, D., Decker, W.K., Sacchetti, B., Funari, A., Michienzi, S., Cesare, S Di, Piersanti, S., Saggio, I., Tagliafico, E., Ferrari, S., Robey, P.G., Riminucci, M., Bianco, P., Sangeetha, V.M., Kale, V.P., Limaye, L.S., Schofield, R., Sharma, M.B., Limaye, L.S., Kale, V.P., Stemple, D.L., Anderson, D.J., Stier, S., Ko, Y., Forkert, R., Lutz, C., Neuhaus, T., Grünewald, E., Cheng, T., Dombkowski, D., Calvi, L.M., Rittling, S.R., Scadden, D.T., Thiemann, F.T., Moore, K.A., Smogorzewska, E.M., Lemischka, I.R., Crooks, G.M., Tormin, A., Li, O., Brune, J.C., Walsh, S., Schütz, B., Ehinger, M., Ditzel, N., Kassem, M., Scheding, S., Urbano-Ispizua, A., Rozman, C., Pimentel, P., Solano, C., de la Rubia, J., Brunet, S., Pérez-Oteiza, J., Ferrá, C., Zuazu, J., Caballero, D., Transplantation, S.G., for A.P.B., Verfaillie, C.M., Zhang, C.C., Kaba, M., Ge, G., Xie, K., Tong, W., Hug, C., Lodish, H.F., Zhang, C.C., Kaba, M., Iizuka, S., Huynh, H., Lodish, H.F., Bonzon-Kulichenko, E., Martínez-Martínez, S., Trevisan-Herraz, M., Navarro, P., Redondo, J.M., Vázquez, J., Bonzon-Kulichenko, E., Perez-Hernandez, D., Nunez, E., Martinez-Acedo, P., Navarro, P., Trevisan-Herraz, M., Mdel, C.R., Sierra, S., Martinez-Martinez, S., Ruiz-Meana, M., Jorge, I., Navarro, P., Martínez-Acedo, P., Núñez, E., Serrano, H., Alfranca, A., Redondo, J.M., Vázquez, J., Martínez-Bartolomé, S., Navarro, P., Martín-Maroto, F., López-Ferrer, D., Ramos-Fernández, A., Villar, M., García-Ruiz, J.P., Vázquez, J., Navarro, P., Vázquez, J., Ramos-Fernández, A., López-Ferrer, D., Vázquez, J., 2013. Self-renewing human bone marrow mesenspheres promote hematopoietic stem cell expansion. Cell Rep. 3, 1714–1724. https://doi.org/10.1016/j.celrep.2013.03.041.

Krampera, M., Pasini, A., Rigo, A., Scupoli, M.T., Tecchio, C., Malpeli, G., Scarpa, A., Dazzi, F., Pizzolo, G., Vinante, F., 2005. HB-EGF/HER-1 signaling in bone marrow mesenchymal stem cells: Inducing cell expansion and reversibly preventing multilineage differentiation. Blood 106, 59–66. https://doi.org/10.1182/blood-2004-09-3645.

Krebsbach, P.H., Villa-Diaz, L.G., 2017. The role of integrin α6 (CD49f) in stem cells: more than a conserved biomarker. scd.2016.0319. Stem Cells Dev. https://doi.org/10.1089/scd.2016.0319.

Lee, M.W., Kim, D.S., Yoo, K.H., Kim, H.R., Jang, I.K., Lee, J.H., Kim, S.Y., Son, M.H., Lee, S.H., Jung, H.L., Sung, K.W.S., Koo, H.H.K., 2013. Human bone marrow-derived mesenchymal stem cell gene expression patterns vary with culture conditions. Blood Res. 48, 107–114. https://doi.org/10.5045/br.2013.48.2.107.

Lee, R.H., Seo, M.J., Pulina, A., Gregory, C., Ylostalo, J., Prockop, D.J., 2009. The CD34-like protein PODXL and {alpha}6-integrin (CD49f) identify early progenitor MSCs with increased clonogenicity and migration to infarcted heart in mice. Blood 113, 816–826. https://doi.org/10.1182/blood-2007-12-128702.

Liu, Z.-J., Zhuge, Y., Velazquez, O.C., 2009. Trafficking and differentiation of mesenchymal stem cells. J. Cell. Biochem. 106, 984–991. https://doi.org/10.1002/jcb.22091.

Marthaler, A.G., Adachi, K., Tiemann, U., Wu, G., Sabour, D., Velychko, S., Kleiter, I., Schöler, H.R., Tapia, N., 2016. Enhanced OCT4 transcriptional activity substitutes for exogenous SOX2 in cellular reprogramming. Sci. Rep. 6, 1–7. https://doi.org/10.1038/srep19415.

Martínez-Conesa, E.M., Espel, E., Reina, M., Casaroli-Marano, R.P., 2012. Characterization of ocular surface epithelial and progenitor cell markers in human adipose stromal cells derived from lipoaspirates. Invest. Ophthalmol. Vis. Sci. 53, 513–520. https://doi.org/10.1167/iovs.11-7550.

Matic, I., Antunovic, M., Brkic, S., Josipovic, P., Caput Mihalic, K., Karlak, I., Ivkovic, A., Marijanovic, I., 2016. Expression of OCT-4 and SOX-2 in bone marrow-derived human mesenchymal stem cells during osteogenic differentiation. Open Access Maced. J. Med. Sci. 4, 9–16. https://doi.org/10.3889/oamjms.2016.008.

Mosna, F., Sensebé, L., Krampera, M., 2010. Human bone marrow and adipose tissue mesenchymal stem cells: a user's guide. Stem Cells Dev. 19, 1449–1470. https://doi.org/10.1089/scd.2010.0140.

Orkin, S.H., Wang, J., Kim, J., Chu, J., Rao, S., Theunissen, T.W., Shen, X., Levasseur, D. N., 2008. The transcriptional network controlling pluripotency in ES cells. In: Cold Spring Harbor Symposia on Quantitative Biology. doi:10.1101/sqb.2008.72.001.

Piera-Velazquez, S., Jimenez, S.A., Stokes, D.G., 2002. Increased life span of human osteoarthritic chondrocytes by exogenous expression of telomerase. Arthritis Rheum. 46, 683–693. https://doi.org/10.1002/art.10116.

Pierantozzi, E., Gava, B., Manini, I., Roviello, F., Marotta, G., Chiavarelli, M., Sorrentino, V., 2011. Pluripotency regulators in human mesenchymal stem cells: expression of NANOG but not of OCT-4 and SOX-2. Stem Cells Dev. 20, 915–923. https://doi.org/10.1089/scd.2010.0353.

Qian, H., Tryggvason, K., Jacobsen, S.E., Ekblom, M., 2006. Contribution of alpha6 integrins to hematopoietic stem and progenitor cell homing to bone marrow and collaboration with alpha4 integrins. Blood 107, 3503–3510. https://doi.org/10.1182/blood-2005-10-3932.

Rasband, W., 2012. ImageJ. U. S. Natl. Institutes Heal. Bethesda, Maryland, USA //imagej.nih.gov/ij/.

R Development Core Team, 2012, version 3.1.1, https://cran.r-roject.org/bin/windows/base/old/3.1.1/.

Ridera, D., Dombrowski, C., Sawyer, A., Ng, G.H.B., Leong, D., Hutmacher, D.W., Nurcombe, V., Cool, S.M., 2008. Autocrine fibroblast growth factor 2 increases the multipotentiality of human adipose-derived mesenchymal stem cells. Stem Cells 26, 1598–1608. https://doi.org/10.1634/stemcells.2007-0480.

Rizzino, A., 2013. Interdependent network integrated at multiple levels. Stem Cells 31, 1033–1039. https://doi.org/10.1002/stem.1352.The.

Rodríguez, M.D.C., Bernad, A., Aracil, M., 2004. Interleukin-6 deficiency affects bone marrow stromal precursors, resulting in defective hematopoietic support. Blood 103, 3349–3354. https://doi.org/10.1182/blood-2003-10-3438.

Romano, A.C., Espana, E.M., Yoo, S.H., Budak, M.T., Wolosin, J.M., Tseng, S.C.G., 2003. Different cell sizes in human limbal and central corneal basal epithelia measured by confocal microscopy and flow cytometry. Investig. Ophthalmol. Vis. Sci. 44, 5125–5129. https://doi.org/10.1167/iovs.03-0628.

Shangguan, L., Ti, X., Krause, U., Hai, B., Zhao, Y., Yang, Z., Liu, F., 2012. Inhibition of TGF-β/Smad signaling by BAMBI blocks differentiation of human mesenchymal stem cells to carcinoma-associated fibroblasts and abolishes their protumor effects. Stem Cells 30, 2810–2819. https://doi.org/10.1002/stem.1251.

Sotiropouloua, P., Perez, S., Salagianni, M., Baxevanis, C.N., Papamichail, M., 2006. Characterization of the optimal culture conditions for clinical scale production of human mesenchymal stem cells. Stem Cells 24, 462–471. https://doi.org/10.1634/stemcells.2004-0331.

Squillaro, T., Peluso, G., Galderisi, U., 2016. Clinical trials with mesenchymal stem cells: an update. Cell Transplant. https://doi.org/10.3727/096368915X689622.

Tamama, K., Fan, V.H., Griffith, L.G., Blair, H.C., Wells, A., 2006. Epidermal growth factor as a candidate for ex vivo expansion of bone marrow-derived mesenchymal stem cells. Stem Cells. https://doi.org/10.1634/stemcells.2005-0176.

Ullah, M., Liu, D.D., Thakor, A.S., 2019. Mesenchymal stromal cell homing: mechanisms and strategies for improvement. iScience. doi:10.1016/j.isci.2019.05.004.

Villa-Diaz, L.G., Kim, J.K., Laperle, A., Palecek, S.P., Krebsbach, P.H., 2016. Inhibition of focal adhesion kinase signaling by integrin α6β1 supports human pluripotent stem cell self-renewal. Stem Cells 34, 1753–1764. https://doi.org/10.1002/stem.2349.

Yu, K.R., Yang, S.R., Jung, J.W., Kim, H., Ko, K., Han, D.W., Park, S.B., Choi, S.W., Kang, S.K., Schöler, H., Kang, K.S., 2012. CD49f enhances multipotency and maintains stemness through the direct regulation of OCT4 and SOX2. Stem Cells 30, 876–887. https://doi.org/10.1002/stem.1052.

Zaim, M., Karaman, S., Cetin, G., Isik, S., 2012. Donor age and long-term culture affect differentiation and proliferation of human bone marrow mesenchymal stem cells. Ann. Hematol. 91, 1175–1186. https://doi.org/10.1007/s00277-012-1438-x.

Zhang, S., Liu, P., Chen, L., Wang, Y., Wang, Z., Zhang, B., 2015. The effects of spheroid formation of adipose-derived stem cells in a microgravity bioreactor on stemness properties and therapeutic potential. Biomaterials 41, 15–25. https://doi.org/10.1016/j.biomaterials.2014.11.019.

Zhu, M., Kohan, E., Bradley, J., Hedrick, M., Benhaim, P., Zuk, P., 2009. The effect of age on osteogenic, adipogenic and proliferative potential of female adipose-derived stem cells. J. Tissue Eng. Regen. Med. 3, 290–301. https://doi.org/10.1002/term.165.